

# LLRF Design for the HINS-SRF Test Facility at Fermilab\*

J. Branlard<sup>†</sup>, B. Chase, E. Cullerton, P. Joireman, V. Tupikov  
Fermi National Accelerator Laboratory, Batavia, IL, U.S.A.

## Abstract

The High Intensity Neutrino Source (HINS) R&D program requires super conducting single spoke resonators operating at 325 MHz (SSR1) [1]. After coupler installation, these cavities are tested at the HINS-SRF facility at Fermilab. The LLRF requirements for these tests include support for continuous wave and pulsed mode operations, with the ability to track the resonance frequency of the tested cavity. Real-time measurement of the cavity loaded  $Q$  and  $Q_0$  are implemented using gradient decay techniques, allowing for  $Q_0$  versus  $E_{acc}$  plots. A real time cavity simulator was also developed to test the LLRF system and verify its functionality.

## LLRF SYSTEM OVERVIEW

The LLRF system is depicted in Fig. 1. The 325 MHz RF reference is provided by a signal generator (Aeroflex IFR 2023A), for tunability. The master oscillator and local oscillator chassis distributes the 325 MHz reference signal and generates the 338 MHz LO. The LO is obtained by mixing the 325 MHz RF signal with a 13 MHz intermediate frequency (IF), internally generated by dividing the 325 MHz reference by 25. This allows the LO to track the RF signal when it is tuned to match the cavity resonance frequency.

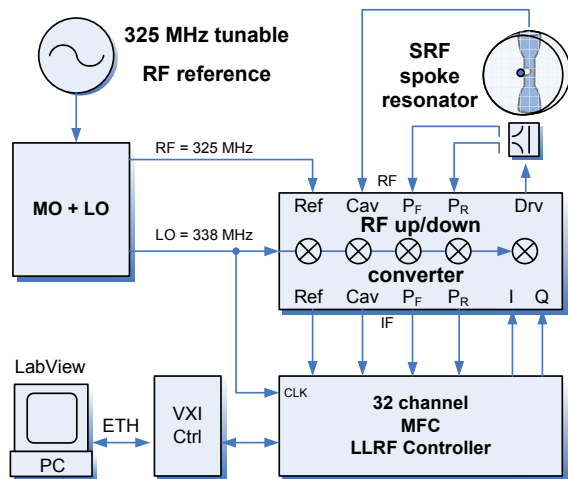


Figure 1: Overview of the LLRF system.

The 8 channel receiver / 1 channel transmitter [2] previously developed for Fermilab 1.3 GHz SRF test facilities

\* Work supported by Fermi Research Alliance, LLC, under Contract No. DE-AC02-07CH11359 with the United States Department of Energy

<sup>†</sup> branlard@fnal.gov

was modified to operate at RF=325 MHz with a 338 MHz LO. The down conversion has a +13 dBm 1-dB compression point at the RF input, the conversion loss is -4 dB and the channel to channel isolation is better than -80 dB. For this test, only 4 out of 8 available channels are used to down convert the 325 MHz reference, the cavity probe, forward and reflected power signals. The down converter has a 21 dB noise figure and the transmitter has an output noise of -138 dBm/ $\sqrt{\text{Hz}}$  at 325 MHz. A single side band up converter section is used to generate the RF drive signal to the cavity from quadrature IF signals. The IF signals are directed to and from the multi cavity field controller board (MFC) [3], previously developed at Fermilab for ILCTA projects. The MFC has 32 12-bit ADCs and 4 14-bit DACs, a Cyclone II FPGA and a SHARC DSP. The firmware was modified to operate in continuous wave (CW) with a 338 MHz clock. The FPGA clock runs at 56.33 MHz (338 MHz  $\div$  6) and the controller has an internal latency around 800ns. Low level C libraries and a LabView interface were developed to communicate with the board through the VXI controller. The drive output of the converter is sent to a dual directional power coupler (NARDA 3020A) at the input of the cavity. This 20 dB coupler has a minimum directivity of 35 dB and a VSWR of 1.05.

## FREQUENCY TRACKING AND CAVITY SIMULATOR

The super conducting cavities to be tested in the Horizontal Test Stand (HTS) are expected to have  $Q_0 \approx 10^9$  and  $Q_L \approx 10^8$ . Frequency tuners have been installed [4] but the preliminary tests assume no control of the cavity resonance frequency. For this reason, the LLRF system was modified to track the cavity resonance frequency. The principle of the LLRF frequency tracking system is explained next. To test its functionality, a cavity simulator was also developed, as explained in the following section.

### Frequency Tracking

The cavities to be tested at HTS have a resonance frequency centered at 325 MHz  $\pm$  200 kHz. During operations, the center frequency should not drift by more than  $\pm$  20 kHz depending on the gradient. To handle the resonance frequency discrepancies from one cavity to the next, the 325 MHz RF reference frequency is tuned manually to bring the RF close (i.e. within  $\pm$  20 kHz) to the cavity resonance frequency. This "coarse" tuning remains unchanged for cavity operations until the next cavity is tested. To handle the "fine" frequency fluctuations, a digital phase lock loop (PLL) was implemented, detecting the phase of

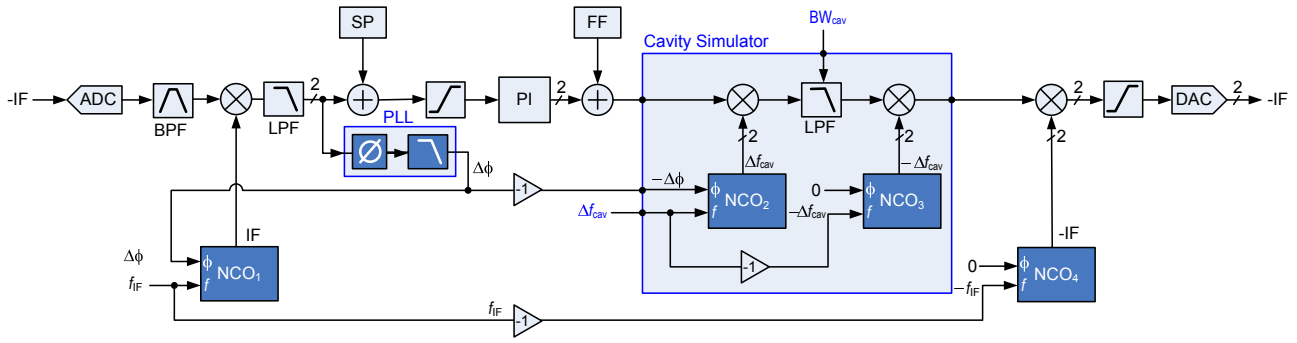


Figure 2: FPGA signal flow with IF up and down conversion and cavity simulator

the base band cavity signal as illustrated in Fig. 2. The PLL phase error  $\Delta\Phi$  is integrated at the first Numerical Controlled Oscillator (NCO<sub>1</sub>) as a frequency shift. It results that NCO<sub>1</sub> always brings the cavity signal to base band and tracks the cavity frequency during operations. The PLL loop filter was designed with a 400 kHz bandwidth but the phase corrections are clamped to 40 kHz to account for the expected  $\pm 20$  kHz cavity detuning. A CORDIC is used in the PLL to detect the cavity phase and reduce its signal amplitude sensitivity. Note that the phase error  $\Delta\Phi$  is not applied at the digital up conversion (NCO<sub>4</sub>), to preserve the PLL frequency correction.

### Cavity Simulator

To simulate cavities with bandwidths as low as 0.1 Hz, an efficient cavity simulator was implemented. A band pass filter implementation for such narrow band cavities would require too many multipliers in the on-board FPGA. Instead, a combination of a low pass filter in series with 2 complex multipliers was used as illustrated in Fig. 2.

The low pass filter cut-off frequency ( $BW_{cav}$ ) determines the 3 dB pass band of the cavity and the frequency input to the 2 NCOs performing the up and down conversion from base band ( $\Delta f_{cav}$ ) sets the cavity detuning. In Fig. 2, NCO<sub>2</sub> translates the base band cavity signal by the cavity detuning frequency  $\Delta f_{cav}$ , while NCO<sub>3</sub> brings the cavity signal back to base band. NCO<sub>2</sub> and NCO<sub>3</sub> perform opposite frequency translations, hence the sign inversion for their frequency request input. The phase error from the frequency tracking is only applied to the first NCO of the cavity simulator (NCO<sub>2</sub>). This phase error translates as amplitude attenuation and phase shift in the cavity simulator, in turn detected as a frequency shift by the PLL. Also applying the phase correction  $\Delta\Phi$  to NCO<sub>3</sub> would annul the phase shift and break the frequency tracking mechanism. The IF quadrature DAC outputs are then used to drive the analog up converter. The resulting 325 MHz RF drive is looped back to the receiver section into the cavity probe RF input, as illustrated in Fig. 3. This efficient cavity simulator implementation proved to be very useful to troubleshoot control algorithms and provided a reliable substitute to the RF cavity when it was not available or operational.

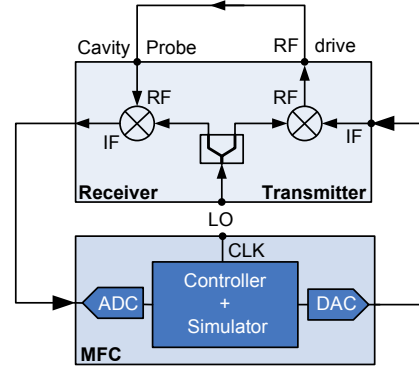


Figure 3: Signal flow of the real-time cavity simulator.

## MEASUREMENTS

While the LLRF system was designed to handle both continuous wave (CW) and pulsed mode operation, initial tests with SSR1 have been conducted in CW mode. Real-time measurements of different cavity parameters ( $Q_0$ ,  $Q_L$ ,  $Q_e$  and  $Q_t$ ) are implemented in a LabView interface for CW operations.

The first step for these real-time calculations consists of performing a decay measurement, typically done at low gradient (1-3 MV/m) to avoid multi-pacting. From a steady-state operating point, the RF drive is disabled to generate an amplitude decay. The decay of the cavity probe signal is sampled at 20-30 Hz and recorded. The RF is re-enabled when the decayed probe reading is 95-99% of the initial steady-state gradient. For a cavity with a bandwidth of 0.1 Hz, this corresponds to 300-400 points. Assuming an exponential decay, the natural logarithm of the decay is calculated, a least mean square linear fit is found and the cavity loaded Q is derived from the linear fit slope. The time samples are denoted as  $x[n]$  and  $y[n] = \ln(V_{cav}[n])$ ,  $\sigma_{xx}^2$  and  $\sigma_{xy}^2$  indicate the corresponding variance and covariance. The cavity time constant is then obtained using  $\tau = -\sigma_{xx}^2 / \sigma_{xy}^2$  and the corresponding loaded quality factor is given by:

$$Q_L = \frac{\omega_0 \tau}{2} = -\frac{\omega_0}{2} \times \frac{\sigma_{xx}^2}{\sigma_{xy}^2} \quad (1)$$

For over-coupled cavities, the external (or input coupler) quality factor,  $Q_e$  and the transmitted (or probe) quality factor,  $Q_t$  are calculated with the following formulae [5, 6]:

$$Q_e = \frac{2Q_L}{1 + \sqrt{\frac{P_R}{P_F}}} \quad (2)$$

$$Q_t = \frac{2Q_L}{1 + \sqrt{\frac{P_R}{P_F}}} \times \frac{2P_F - P_R}{P_T} \quad (3)$$

where,  $P_F$ ,  $P_R$  and  $P_T$  are respectively the forward, reflected and transmitted powers, calibrated in Watts. The cavity unloaded quality factor  $Q_0$  and voltage  $V_{\text{cav}}$  can be calculated using

$$Q_0 = \left( \frac{1}{Q_L} - \frac{1}{Q_e} - \frac{1}{Q_t} \right)^{-1} \quad (4)$$

$$V_{\text{cav}} = \sqrt{R/Q \times P_{\text{loss}} Q_0} \quad (5)$$

where  $P_{\text{loss}} = P_F - P_R - P_T$  is the power loss to the cavity walls. Finally, the cavity voltage scaling coefficient  $k_T$  is calculated:

$$k_T = \frac{V_{\text{cav}}}{\sqrt{P_T}} \quad (6)$$

Once calculated during the decay measurements,  $Q_e$ ,  $Q_t$  and  $k_T$  are then assumed to remain constant regardless of the gradient of operation and their calculated values are saved until the next decay measurement. During steady state operations (i.e. outside from decay transients), the cavity voltage, unloaded Q and loaded Q are recalculated in real time as a function of the instantaneous power readings,  $P_F$ ,  $P_R$  and  $P_T$ :

$$V_{\text{cav}} = k_T \sqrt{P_T} \quad (7)$$

$$Q_0 = \frac{V_{\text{cav}}^2}{R/Q \times P_{\text{loss}}} \quad (8)$$

$$Q_L = \left( \frac{1}{Q_0} + \frac{1}{Q_e} + \frac{1}{Q_t} \right)^{-1} \quad (9)$$

Finally, to minimize the load on the cryogenic system, an amplitude toggling mode was developed, switching back and forth between high gradient and low gradient operations, every 5-10 seconds. This allowed for high gradient measurements while minimizing the impact on the cryogenic system and helped keep the helium pressure stable.

## RESULTS

The plot of Fig. 4 shows the time correlation between the cryovessel pressure fluctuations and the cavity detuning. The cavity pressure sensitivity is found to be  $df/dP \approx 131 \text{ Hz/Torr}$ , (100 Hz/mBar). Without feedback control, the cryovessel helium pressure fluctuates by  $\approx 14 \text{ Torr}$  (19 mBar), which translates to 1.9 kHz of detuning, well within the bandwidth of the LLRF frequency tracking PLL. It would otherwise be impossible to operate a cavity with a 1 Hz bandwidth experiencing such a detuning. Using the decay measurements,  $Q_L \approx 2 \times 10^8$

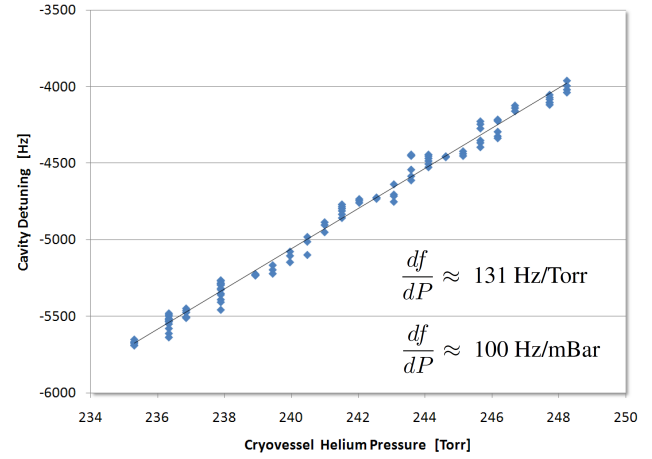


Figure 4: Correlation between the cryovessel pressure and the cavity resonance frequency.

and  $Q_0 \approx 0.4 - 1.4 \times 10^9$  were measured. The gradient dependence of  $Q_0$  was also measured; complete results obtained with the first 325 MHz SRF spoke resonator tested at the HINS horizontal test stand are reported by Webber *et al* [7].

## REFERENCES

- [1] L. Ristori *et al.*, "Design, Fabrication and Testing of Single Spoke Resonators at Fermilab", THPPO011, Proceedings of SRF 2009, Berlin, Germany.
- [2] U. Mavrič *et al.*, "A 96 channel receiver for the ILCTA LLRF system at Fermilab", Proceedings of PAC07, 2007, Albuquerque, New Mexico, USA.
- [3] P. Varghese *et al.*, "Multichannel Vector Field Control Module for LLRF Control of Superconducting Cavities", Proceedings of PAC07, 2007, Albuquerque, New Mexico, USA.
- [4] Y. Pischalnikov *et al.*, "A tuner for a 325 MHz SRF spoke cavity", THPPO043, Proceedings of SRF 2009, Berlin, Germany.
- [5] H. Padamsee, J. Knobloch, T. Hays, "RF Superconductivity for Accelerators", Wiley Series in Beam Physics and Accelerator Technology.
- [6] T. Powers, "Theory and Practice of Cavity RF Test Systems", 12th International Workshop on RF Superconductivity, Ithaca, NY, USA, 2005.
- [7] R. Webber *et al.*, "First High Gradient Test Results of a 325 MHz Superconducting Single Spoke Resonator with Helium Vessel at Fermilab", THP031, Linac 2010 Proceedings, Tsukuba, Japan, 2010.